Journal of the Korean Chemical Society
2012, *Vol. 56, No. 4*
Printed in the Republic of Korea
http://dx.doi.org/10.5012/jkcs.2012.56.4.478

Preparation of Fe_3O_4/SiO_2 Core/Shell Nanoparticles with Ultrathin Silica Layer

Eue-Soon Jang*
Department of Applied Chemistry, Kumoh National Institute of Technology, Gyeongbuk 730-701, Korea
**E-mail: euesoon@kumoh.ac.kr*
(Received April 30, 2012; Accepted May 11, 2012)

ABSTRACT. We successfully synthesized Fe_3O_4/SiO_2 nanoparticles with ultrathin silica layer of 1.0±0.5 nm that was fine controlled by changing concentration of Fe_3O_4. Among various reaction conditions for silica coating, increasing concentration of Fe_3O_4 was more effective approach to decrease silica thickness compared to water-to-surfactant ratio control. Moreover, we found that concentration of the 1-octanol is also important factor to produce the homogeneous Fe_3O_4/SiO_2 nanoparticles. The present approach could be available to apply on preparation of other core/shell nanoparticles with ultrathin silica layer.

Key words: Reverse microemulsion procedure, Fe_3O_4/SiO_2 nanoparticles, Silica thickness, Water-to-surfactant ratio, Fe_3O_4 concentration

INTRODUCTION

Thanks to their high magnetic response and biocompatibility, iron oxide (Fe_3O_4) magnetic nanoparticles have received significant interest for biomedical applications in the diagnosis and treatment of various diseases.[1-3] Therefore, various procedures, such as coprecipitation,[4] sol-gel,[5] and polyol methods,[6] have been developed to prepare monodispersed Fe_3O_4 nanoparticles. Among the methods developed, the use of an organic solvent with a high boiling temperature, like 1-octadecene (b.p.=315 ^oC), has been preferred for achieving higher crystallinity and magnetic properties over those achieved by coprecipitation processes based on aqueous media.[7-9] However, the hydrophobic surface of the resulting Fe_3O_4 should be modified to produce water-dispersible nanoparticles for further biomedical applications. While various methods have been reported thus far, the many advantages of silica listed below make it one of the most appropriate materials for modifying Fe_3O_4.[10-12]

(1) It is biocompatible and stable in biological environments;

(2) It reduces the chemical toxicity of the core nanoparticles (e.g., by suppressing the release of toxic Fe^{2+} ions from Fe_3O_4); and

(3) It guarantees the chemical and physical properties of the core nanoparticles by protecting them from the external environment.

Moreover, well-known silane chemistry allows us to prepare Fe_3O_4/SiO_2 core/shell nanoparticles with various reaction active sites, with functional groups such as amines, carboxylates, and thiols, through silane coupling reactions and we can thus easily synthesize multifunctional nanoparticles.[13] Consequently, various silica-based core/shell nanostructures with multimodality have been investigated for molecular imaging and nanomedicine applications.[1,10-13] The Stöber method is the most commonly used procedure for obtaining silica-coated nanoparticles due to its simplicity in using hydrophilic ethanol solvent.[1,14] However, achieving thickness control below 50 nm by this method is difficult and thus the particle sizes of the core/shell nanoparticles increase up to the submicrometer scale.[15,16] Such large particles could lead to serious problems in renal clearance and cytotoxicity due to the long blood circulation time and their extensive accumulation into the liver, spleen, and lungs.[17,18] Moreover, the extent of magnetic interactions between the core Fe_3O_4 nanoparticles and an external magnetic field could be reduced by the increased thickness of the SiO_2 layer due to the intrinsically diamagnetic property of the silica material. In fact, we have previously found that the 1/T(2) relaxivity of the core Fe_3O_4 is significantly reduced by an increase in the silica thickness.[19] Therefore, technology with a thin layer of silica coating is very important for the biomedical application of silica-based core/shell nanoparticles. A reverse microemulsion procedure satisfies the purpose of preparing thin silica layer-coated Fe_3O_4/SiO_2 nanoparticles.[20,21]

In this study, we demonstrate the optimal conditions for a reverse microemulsion procedure for the preparation of

Fe_3O_4/SiO_2 nanoparticles with an ultrathin silica layer that can be controlled to a thickness of 1.0 nm. Such an ultrathin silica layer is a notable result because the average thickness of silica layers previously prepared by reverse microemulsion has been reported as 10-70 nm.[20-23] Moreover, we find that the SiO_2 thickness control mechanism is different from that for pure silica nanoparticles.

EXPERIMENTAL

Oleic acid-coated Fe_3O_4 nanoparticles (13±2.5 nm in diameter) were provided by Ocean Nanotech LLC. The concentration of the supplied Fe_3O_4 nanoparticles was determined by inductively coupled plasma analysis as being 22.9 Fe mg/mL. Silica coating of the Fe_3O_4 nanoparticles was accomplished by a modified reverse microemulsion procedure. In a typical synthesis, 5-300 μL of bare Fe_3O_4 nanoparticles were suspended in 29.2 mL of cyclohexane (Aldrich) under mild stirring conditions and then 50-100 mM Triton-X100 (Aldrich) and 29.4-88.3 μM NH_4OH (29.3 wt%, Aldrich) were added to the solution. The clear dark brown solution changed to being a turbid solution by the addition of NH_4OH. The stable reverse microemulsion was generated by adding 0.04-0.22 M 1-octanol such that the resulting solution became optically transparent. Addition of 165 mM tetraethyl orthosilicate (TEOS) to the solution resulted in the immediate hydrolysis of the TEOS. Then, the growing of the silica layer (through condensation reaction) was continued by vigorous stirring (600 rpm) for 72 h at room temperature. The reaction was terminated by adding acetone solvent before the excess organic residents were removed through centrifugation at 15,000 rpm for 30 min. The precipitated Fe_3O_4/SiO_2 core/shell nanoparticles were redispersed into ethanol solvent by sonication.

RESULTS AND DISCUSSION

As a template for the hydrolysis and condensation reaction of TEOS, the stable formation of reverse microemulsions plays a central role in the silica coating of the core nanoparticles that could be achieved by additional surfactants and NH_4OH. In the present study, we used Triton-X100 (TX 100) as the main surfactant and 1-octanol as a helper surfactant. In addition, formation of the reverse microemulsion could be completed by NH_4OH as the supplier of both the reactant (H_2O) and catalyst (NH_3) for the hydrolysis of TEOS. The effects of such reactants on the formation of pure silica nanoparticles without core materials has been well established by Arriagada and Osseo-Asare.[24,25] More particularly, they showed that the particle size of the silica nanoparticles was sensitive to changes in the water-to-surfactant molar ratio (W/S). They considered only the surfactant associated with the reverse micelles formation, without the freely dispersed surfactant in the organic solvent. In contrast, we have used a simplified W/S molar ratio that includes the total concentration of the surfactant, such as in the following expression.

$$W/S=[H_2O]/[TX100]$$

Although the definition of [surfactant] in the present W/S ratio is different from that reported previously, any discrepancy between the two different W/S ratios is negligible because the concentration of the free TX-100 surfactant in the oil phase is constant at the given temperature and solvent. We added no additional deionized water; therefore, the quantity of H_2O was controlled by the concentration of NH_4OH, i.e., we considered that 70.7 wt% of the added 29.3 wt% [NH_4OH] was [H_2O].

Most previous reports have investigated the influence of [TX-100] on the formation of the silica nanoparticles, but studies on helper surfactants like 1-octanol have only rarely been reported upon thus far.[24-27] As shown in *Fig.* 1(a), the bare Fe_3O_4 nanoparticles have a uniform size of 13 nm. *Figs.* 1(b)-(f) show the changes in the silica layer upon variation of [1-octanol], but the W/S ratio, [Fe_3O_4], and [TEOS] were fixed at 3, 16.9 μM, and 16.4 mM, respectively. When [1-octanol] was altered to 0.22, 0.13, and 0.04 M, we observed a slight decrease in the average size of the Fe_3O_4/SiO_2 nanoparticle products, from 121.3 nm to 101.5 nm, as shown in *Figs.* 1(b)-(d). Therefore, the distribution of the silica layer thickness was 54.2±12.0 nm, 43.5±12.8 nm, 42.3±10.8 nm, respectively. However, Fe_3O_4/SiO_2 nanoparticles of heterogeneous size were obtained from the reaction conditions of 0.03 M 1-octanol, as shown in *Fig.* 1(e). From the magnified image in *Fig.* 1(f), we found that small particles have a silica layer thickness of 4.7±1.5 nm. However, the solution for 0.03 M 1-octanol was turbid compared to the optically transparent solutions obtained by the other reaction conditions. This indicates that the [1-octanol] is important for forming a homogeneous silica layer but that a [1-octanol] above a certain concentration does not have a serious effect on the silica thickness. From the above results, we found that the minimum [1-octanol] is approximately 0.04 M in the present study. Therefore, the concentration of 1-octanol was fixed at 0.04 M for the remaining experiments.

According to Osseo-Asare and Arriagada, the silica par-

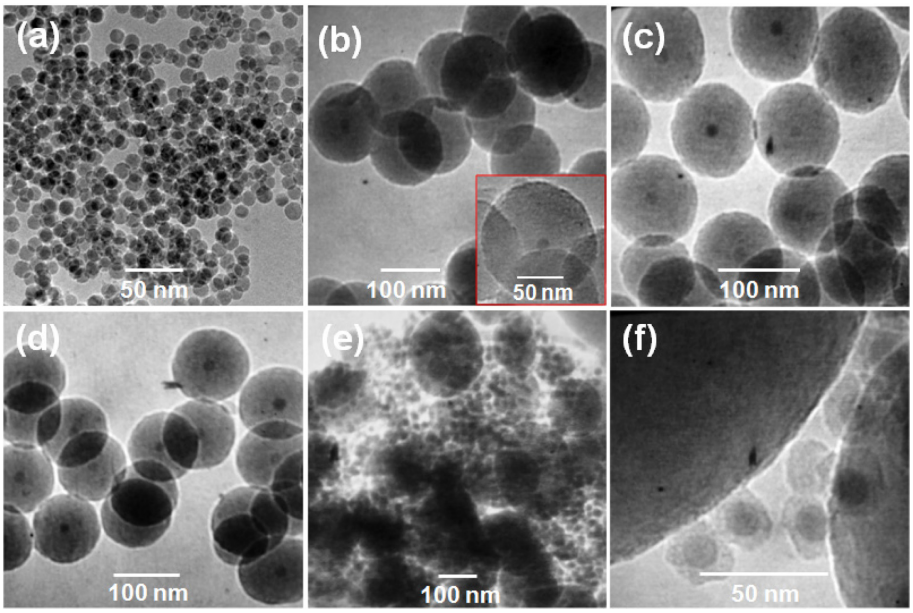

***Fig.* 1.** TEM images of (a) bare Fe_3O_4 and (b-f) Fe_3O_4/SiO_2 nanoparticles obtained from reactant solutions with different [1-octanol]: (b) 0.22 M, (c) 0.13 M, (d) 0.04 M, and (e and f) 0.03 M.

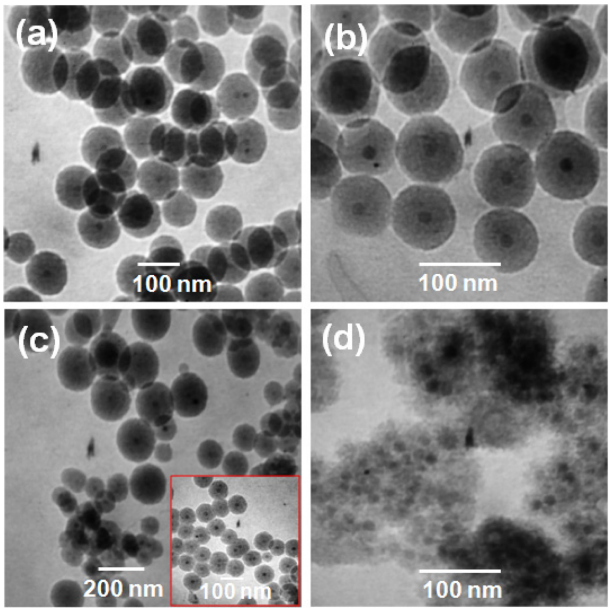

***Fig.* 2.** TEM images of Fe_3O_4/SiO_2 nanoparticles obtained from reactant solutions with different W/S ratios of (a) 3, (b) 2, (c) 1, and (d) 0.5.

ticle size decreases and the size distribution narrows when the W/S ratio is increased from 0.7 to 2.3.[24,25] To test whether a silica layer coated onto Fe_3O_4 nanoparticles shows a similar tendency, we investigated the effect of the W/S ratio on the thickness of the silica layer and particle size distribution. *Figs.* 2(a)-(d) show the variation in the silica layer upon a decreasing W/S ratio (from 3 to 0.5) but with a maintained [Fe_3O_4], [TEOS], and [1-octanol] at 33.9 μM, 165.0 mM, and 40.0 mM, respectively. When the W/S ratio was decreased from 3 to 2, the particle size distribution and silica layer thickness were reduced to 38.6±9.2 nm to 32.8±4.5 nm, as shown in *Figs.* 2(a) and (b). This is consistent with results previously reported.[24,25] However, the size distribution of the Fe_3O_4/SiO_2 nanoparticles for the W/S ratio of 1 broadened due to the cogeneration of large (148.6±12.5 nm) and small (66.9±20.4 nm) Fe_3O_4/SiO_2 nanoparticles, as shown in *Fig.* 2(c). When the W/S ratio was decreased to 0.5, we observed the amorphous silica-coated Fe_3O_4 nanoparticles shown in *Fig.* 2(d). This result implies that the tendency for silica formation on the core nanoparticles is different from that for pure silica nanoparticles without the core materials.[24,25,27]

From the above results, we determined that a [1-octanol] and W/S ratio of 0.04 M and 2, respectively, produce Fe_3O_4/SiO_2 nanoparticles with a homogeneous particle size. However, further optimization of the conditions was required to prepare Fe_3O_4/SiO_2 nanoparticles with a silica layer of thinner thickness. As the next step, we investigated the variation of the silica layer thickness upon changes in [Fe_3O_4] to prepare ultrathin layered Fe_3O_4/SiO_2 nanoparticles. As shown in *Figs.* 3(a)-(e), we found that the silica layer thickness dramatically decreased from 41.0±7.3 to 1.0±0.5 nm upon an increase in [Fe_3O_4] from 16.9 μM to 1.02 mM. The most significant change in the silica layer thickness was observed by increasing [Fe_3O_4] from 101.6

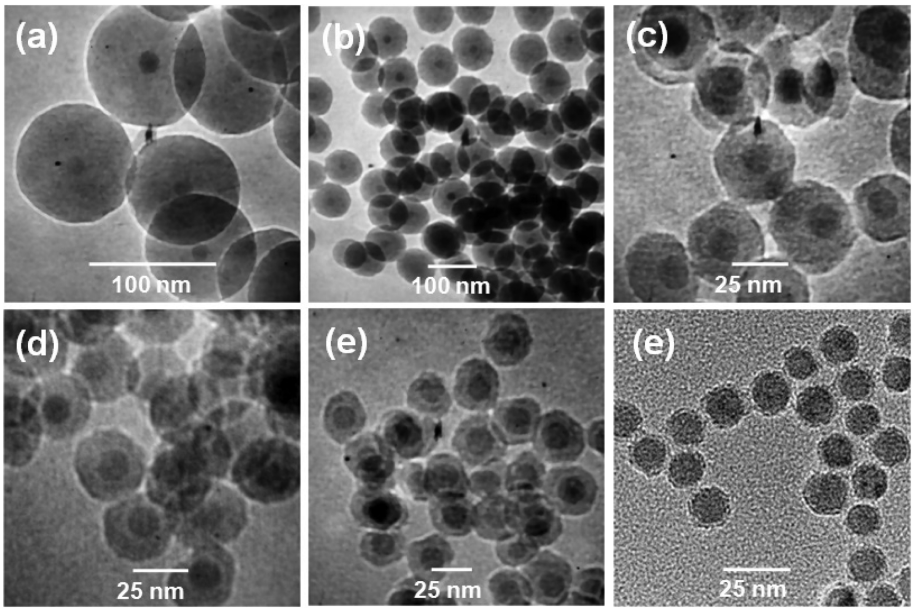

***Fig.* 3.** TEM images of Fe_3O_4/SiO_2 nanoparticles obtained with different $[Fe_3O_4]$: (a) 16.9 mM, (b) 33.9 mM, (c) 101.6 mM, (d) 169.4 mM, (e) 338.7 mM, and (f) 1016.2 mM.

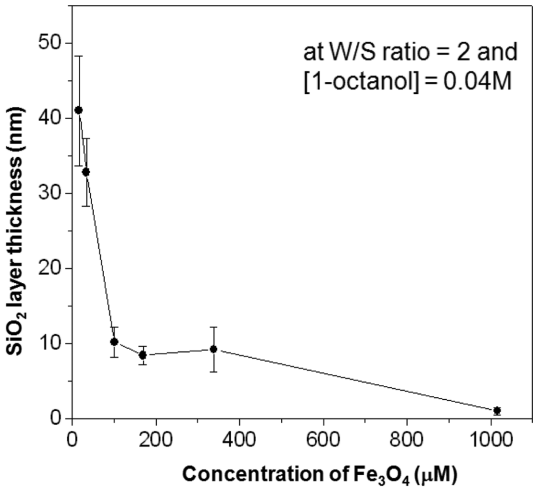

***Fig.* 4.** Variation of silica layer thickness and distribution upon changing $[Fe_3O_4]$.

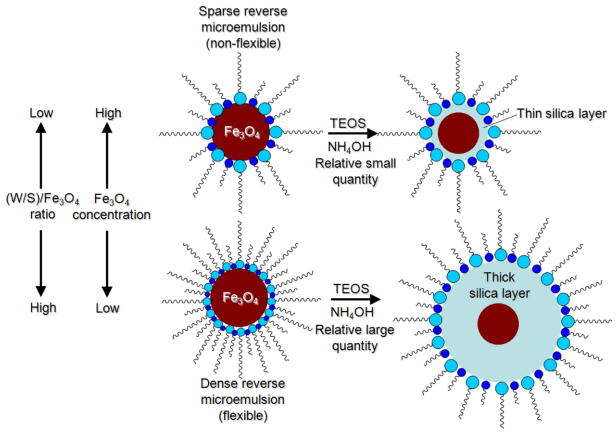

***Scheme* 1.** Schematic representation of the formation of different reverse microemulsion templates at high and low concentrations of Fe_3O_4.

μM to 169.4 μM, as summarized in *Fig.* 4. From the above results, we believe that increasing $[Fe_3O_4]$ is a more effective approach to reduce the silica thickness than is controlling the W/S ratio. *Scheme* 1 demonstrates the reason behind the variation in the silica thickness upon changes in $[Fe_3O_4]$. When $[Fe_3O_4]$ is increased, the $(W/S)/[Fe_3O_4]$ ratio is decreased at a constant W/S ratio. This fact indicates that relatively low concentrations of H_2O and surfactants could lead to the formation of a sparse reverse microemulsion due to the insufficient amount of surfactant. The sparse reverse microemulsion template in the oil phase is relatively non-flexible compared to the dense reverse microemulsion created as a result of the high $(W/S)/[Fe_3O_4]$ ratio, resulting in shrinkage of the reverse microemulsion. Therefore, the sparse reverse microemulsion only allows a small space for silica layer formation *via* hydrolysis and condensation reaction of TEOS. For the large $(W/S)/[Fe_3O_4]$ ratio, the dense reverse microemulsion template is more flexible and thus swelling templates could provide sufficient space for the formation of a large silica layer. Among the two surfactants, the [1-octanol] could have more effect on the flexibility of the templates than TX-100 because the linear hydrocarbon chain of 1-

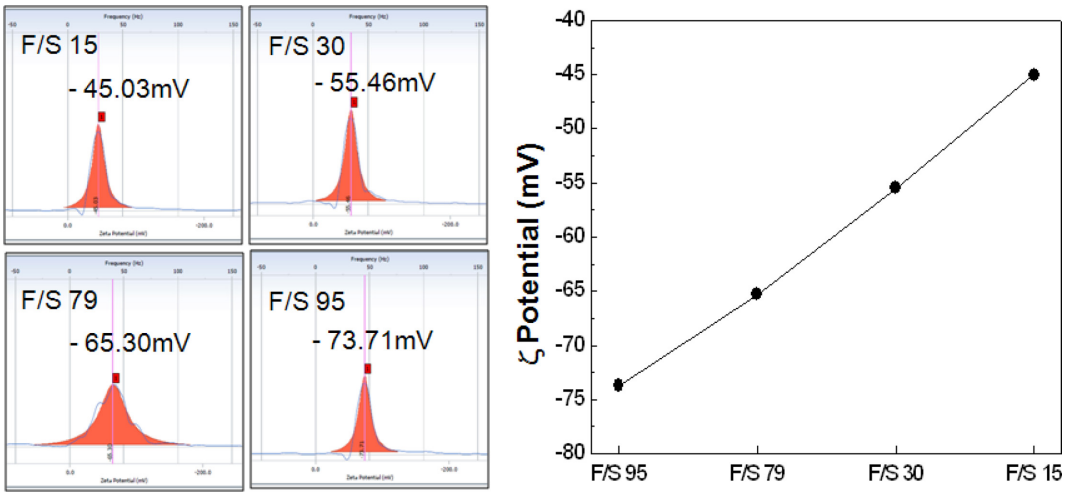

***Fig.* 5.** ζ potential results of Fe_3O_4/SiO_2 (F/S) nanoparticles with different silica thicknesses. The numbers 95, 79, 30, and 15 indicate the average particle size determined from TEM observations.

octanol is more flexible than the rigid phenol group in TX-100. This therefore leads to an understanding of why mixtures of large and small Fe_3O_4/SiO_2 nanoparticles could be generated from 1-octanol concentrations below 0.04 M, as described above.

On the other hand, a thick silica layer coating leads to an increase in the strongly negative surface charge on the Fe_3O_4/SiO_2 nanoparticles through deprotonation of the silanol group (-SiOH).[28,29] In fact, general products of silica possess negative charges over the pH range of most natural waters.[29] Therefore, such a negative surface charge will be enhanced by an increase in the silica thickness, which could lead to severe aggregation *via* strong electrostatic interactions between nanoparticles. *Fig.* 5 shows the ζ potential results for the surface charge of the Fe_3O_4/SiO_2 dispersed into the deionized water, which systematically changed from -73.71 to -45.03 mV by decreasing the silica thickness from 41.0±7.3 nm to 1.0±0.5 nm. For the Fe_3O_4/SiO_2 nanoparticles with the thick silica layer, problems related to colloidal stability could be induced by increasing the negative surface charge and particle size. In fact, even the prepared Fe_3O_4/SiO_2 nanoparticles with a diameter of 95 and 79 nm precipitate out after only a few hours in water, but the Fe_3O_4/SiO_2 nanoparticles with the ultrathin silica layer of 1.0±0.5 nm were monodispersed in solvent for a few weeks without any aggregate formation.

CONCLUSION

The silica thickness control reported in previous works was primarily achieved by changing the W/S ratio. As a result of this, the average silica thickness of the resulting core/shell nanoparticles were reported as 10-70 nm.[20-23] In the present study, we successfully synthesized Fe_3O_4/SiO_2 nanoparticles with a silica thickness of 1.0±0.5 nm from 1.02 mM Fe_3O_4. In addition, we found that increasing $[Fe_3O_4]$ is a more effective approach to reduce the silica thickness than is controlling the W/S ratio. Moreover, the concentration of 1-octanol is also an important factor for producing homogeneous Fe_3O_4/SiO_2 nanoparticles. We believe that a thin layer of silica coating is preferred for biomedical applications of these magnetic nanoparticles. The procedure reported herein could also be applied to the preparation of other core/shell nanoparticles with an ultrathin silica layer.

Acknowledgments. This work was supported by research fund (2011-0024700) of the Korean Ministry of Education, Science and Technology (MEST).

REFERENCES

1. Cho, Y.-S.; Yoon, T.-J.; Jang, E.-S.; Hong, K. S.; Lee, S. Y.; Kim, O. R.; Park, C.; Kim, Y.-J.; Yi, G.-C.; Chang, K. *Cancer Lett.* **2010**, *299*, 63.
2. Green, J. J.; Zhou, B. Y.; Mitalipova, M. M.; Beard, C.; Langer, R.; Jaenisch, R.; Anderson, D. G. *Nano Lett.* **2008**, *8*, 3126.
3. Lee, J.-H.; Jang, J.-T.; Choi, J.-S.; Moon, S. H.; Noh, S.-H.; Kim, J.-W.; Kim, J.-G.; Kim, I.-S.; Park, K. I.; Cheon, J. *Nature Nanotech.* **2011**, *6*, 418.
4. Jolivet, J. P.; Chaneac, C.; Tronc, E. *Chem. Commun.* **2004**, *5*, 481.

5. Xu, J.; Yang, H.; Fu, W.; Du, K.; Sui, Y.; Chen, J.; Zeng, Y.; Li, M.; Zou, G.; *J. Magn. Magn. Mater.* **2007**, *309*, 307.
6. Cai, W.; Wan, J. *J. Colloid Interface Sci.* **2007**, *305*, 366.
7. Sun, S.; Zeng, H.; Robinson, D. B.; Raoux, S.; Rice, P. M.; Wang, S. X.; Li, G. *J. Am. Chem. Soc.* **2004**, 126, 273.
8. Bao, N.; Shen, L.; Wang, Y.; Padhan, P.; Gupta, A. *J. Am. Chem. Soc.* **2007**, *129*, 12374.
9. Park, J.; Joo, J.; Kwon, S.; Jang, Y.; Hyeon, T. *Angew. Chem. Int. Ed.* **2007**, *46*, 4630.
10. Jun, B.-H.; Noh, M. S.; Kim, J.; Kim, G.; Kang, H.; Kim, M.-S.; Seo, Y.-T.; Baek, J.; Kim, J.-H.; Park, J.; Kim, S.; Kim, Y.-K.; Hyeon, T.; Cho, M.-H.; Jeong, D. H.; Lee, Y.-S. *Small* **2010**, *6*, 119.
11. Lee, J.-H.; Jun, Y.-W.; Yeon, S.-I.; Shin, J.-S.; Cheon, J.; *Angew. Chem. Int. Ed.* **2006**, *45*, 8160.
12. Zhang, Y.; Pan, S.; Teng, X.; Luo, Y.; Li, G.; *J. Phys. Chem. C* **2008**, *112*, 9623.
13. Louie, A. *Chem. Rev.* **2010**, *110*, 3146.
14. Stöber, W.; Fink, A.; Bohn, E. *J. Colloid Int. Sci.* **1968**, *26*, 62.
15. Kobayashi, Y.; Katakami, H.; Mine, E.; Nagao, D.; Konno, M.; Marzán, L. M. L. *J. Colloid Int. Sci.* **2005**, *283*, 392.
16. Rossi, L. M.; Shi, L.; Quina, F. H.; Rosenzweig, Z. *Langmuir* **2005**, *21*, 4277.
17. Choi, H. S.; Liu, W.; Misra, P.; Tanaka, E.; Zimmer, J. P.; Ipe, B. I.; Bawendi, M. G.; Frangioni, J. V. *Nature Biotech.* **2007**, *25*, 1165.
18. Huang, J.; Bu, L.; Xie, J.; Chen, K.; Cheng, Z.; Chen, X. *ACS Nano* **2010**, *4*, 7151.
19. Cha, E. J.; Jang, E.-S.; Sun, I. C.; Lee, I. J.; Ko, J. H.; Kim, Y. I. *J. Controlled Release* **2011**, *155*, 152.
20. Han, Y.; Jang, J.; Lee, S. S.; Ying, J. Y. *Langmuir* **2008**, *24*, 5842.
21. Yi, D. K.; Lee, S. S.; Papaefthymiou, G. C.; Ying, J. Y. *Chem. Mater.* **2006**, *18*, 614.
22. Kool, R.; Schooneveld, N. M.; Hilhort, J.; Donegá, C. M.; Hart, D. C.; Balaaderen, A.; Vanmaekelbergh, D.; Meijerink, A. *Chem. Mater.* **2008**, *20*, 2503.
23. Kim, J.; Kim, H. S.; Lee, N.; Kim, T.; Kim, H.; Yu, T.; Song, I. C.; Moon, W. K.; Hyeon, T. *Angew. Chem. Int. Ed.* **2008**, *47*, 8438.
24. O.-Asare, K.; Arriagada, F. J. *Colloids & Surf.* **1990**, *50*, 321.
25. Arriagada, F. J.; O.-Asare, K. *J. Colloid Int. Sci.* **1999**, *211*, 210.
26. Chang, C.-L.; Fogler, H. S. *Langmuir* **1997**, *13*, 3295.
27. Li, T.; Moon, J.; Morrone, A. A.; Mecholsky, J. J.; Talham, D. R.; Adair, H. *Langmuir* **1999**, *15*, 4328.
28. Bagwe, R. P.; Hilliard, L. R.; Tan, W. *Langmuir* **2006**, *22*, 4357.
29. Dove, P. M.; Craven, C. M.; *Geochim. et Cosmochim. Acta* **2005**, *69*, 4963.